Journal of Alloys and Compounds 503 (2010) 529–537

Contents lists available at ScienceDirect

Journal of Alloys and Compounds

journal homepage: www.elsevier.com/locate/jallcom

Nitrogen-electronegativity-induced bowing character in ternary zincblende $Ga_{1-x}In_xN$ alloys

Nacir Tit*

Department of Physics, College of Sciences, UAE University, P.O. Box 17551, Al-Ain, United Arab Emirates

ARTICLE INFO

Article history:
Received 1 February 2010
Received in revised form 4 May 2010
Accepted 5 May 2010
Available online 1 June 2010

PACS:
71.15.−m
71.20.Nr
71.55.Eq
78.55.Cr

Keywords:
Band structure
III–V semiconductors
Photoluminescence

ABSTRACT

The origins of the bandgap bowing character in the common-anion ternary cubic $Ga_{1-x}In_xN$ alloys are investigated using the sp^3s^* tight-binding (TB) method, including the spin–orbit coupling effects within the virtual-crystal approximation (VCA) framework. The method is used to calculate the band structure, density of states and charge ionization versus composition and valence-band offsets (VBO). The results are used to model some recently available experimental optical absorption (Abs) and photoluminescence (PL) data. Two unusual characteristics are discussed: (i) unlike the common-anion "direct-bandgap-based" ternary alloys, the GaInN alloys possess a clearly large *bowing* character. This behavior is found to be mainly caused by the electronegativity of nitrogen atoms, whose effects can induce a competition between the cation (Ga and In) atoms to establish a compromised ionization with the increasing indium content; (ii) a single composition-independent *bowing* parameter cannot describe the bandgap behavior. The decrease of *bowing* parameter with the increasing In content is found to be almost linear and likely to be caused by the composition fluctuation due to the large lattice relaxation. The results also show that the VBO between the two constituents is small (VBO < 0.38 eV), consistent with the predictions of the common-anion rule and the state-of-the-art *ab initio* methods.

© 2010 Elsevier B.V. All rights reserved.

1. Introduction

The nitride-based III–V alloys, such as the quaternary GaInNAs alloys (in the dilute nitride regime), have been successfully utilized in the 1.3–1.5 μm wavelength range, which is of great interest in the telecommunication field. However, the tuning of their bandgap energy towards photonic applications remains limited [1,2]. These limitations mainly stem from challenging growth problems, especially when dealing with materials with high lattice-mismatch, such as the nitride alloys. On the other hand, the II–VI semiconductor alloys remain the predominantly used materials in the opto-electronics field (e.g., the ternary and quaternary alloys of the Cd(Zn)Te(Se) family) [3,4]. It has also proven possible to tune the properties of the elementary semiconductor alloys $Si_xGe_{1-x-y}Sn_y$ for a diversity of telecommunication applications [5–7].

A major reason for the exclusion of GaAs-based nitrides from photonic applications is the huge lattice-mismatch (about 23%) between GaAs and GaN bulk materials. This has persuaded many investigators to deal with dilute nitride alloys (i.e., $Ga_{1-y}In_yN_xAs_{1-x}$, with a nitrogen concentration $x \leq 6\%$) [8,9], in order to avoid lattice-distortion problems. The result is an almost exclusive concentration on telecommunication applications for these alloys. In the current decade, the combination of GaN and InN materials (with a lattice-mismatch of about 10%) in fabricated ternary $In_xGa_{1-x}N$ alloys [10,11], InN/GaN multiple-quantum wells (MQWs) [12–15] and InN/GaN quantum dots [16], has broadened the applications of nitrides as to include photonics. The present investigation focuses on studying the properties of the $In_xGa_{1-x}N$ alloys.

From another perspective, understanding of the bandgap behavior in the context of alloy composition is of crucial importance and relevance to device fabrication for specific applications. In general, the bandgaps relevant to the semiconductor alloys adopt one of the following four behaviors: (i) *bowing* behavior, as is found for the common-cation III–V and II–VI alloys [17]; (ii) linear behavior, as in the case of common-anion alloys [18]; (iii) band anti-crossing, as occurs in indirect-bandgap-based alloys (such as $Si_xGe_{1-x-y}Sn_y$[5–7], $Al_xGa_{1-x}As$ [19] and GaP_xAs_{1-x}[20]); and (iv) anomalous behavior, exemplified by the metallization observed in the highly lattice-mismatched nitride $IIIV_{1-x}N_x$ alloys [21–23]; the negative *bowing* behavior seen in the alloys of $In_xGa_{1-x}As$ [24] and $GaSb_xAs_{1-x}$[25]; the anomalous behavior reported for lead chalcogenides [26], where the direct gap is found to be at the L high-symmetry point of the Brillouin zone.

Selected cases of bandgap behaviors in alloys are illustrated in Fig. 1, while Table 1 summarizes the values of *bowing* parameters for the cases of common-cation ternary alloys. In Fig. 1 the solid lines present *bowing* behaviors, whereas the

* Tel.: +971 3 7134441; fax: +971 3 7671291.
E-mail address: ntit@uaeu.ac.ae.

0925-8388/$ – see front matter © 2010 Elsevier B.V. All rights reserved.
doi:10.1016/j.jallcom.2010.05.049

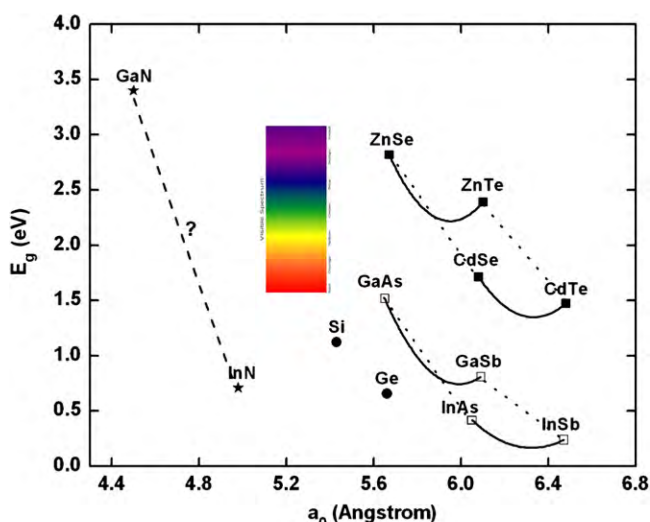

Fig. 1. Variations of bandgap energy versus lattice constant in some special semiconductor ternary alloys.

dotted curves show linear variations. Past investigations have indicated that alloys composed of direct-bandgap (not highly lattice-mismatched) materials possess either the *bowing* behavior when the anion concentration is varied (e.g., the common-cation ternary alloys: $ZnSe_{1-x}Te_x$, $CdSe_{1-x}Te_x$, $GaSb_xAs_{1-x}$ and $InSb_xAs_{1-x}$) [17,27]; or linear behavior, when the cation concentration is varied (e.g., the common-anion ternary alloys: $Zn_{1-x}Cd_xSe$, $Zn_{1-x}Cd_xTe$, $Ga_{1-x}In_xAs$ and $Ga_{1-x}In_xSb$) [18]. The *bowing* character is a manifestation of the competition between anions in trapping the electric charge made available by the cation atoms. This concept explains the results of Ref. [27], which compared the *bowing* character between two common-cation ternary alloys, namely from II–VI and III–V groups. The study by Ref. [27] found that the *bowing* was higher for the II–VI alloys than the III–V alloys, as the former have anion atoms with higher electronegativity (group VI) than the latter (with anions of group V). In the case of common-anion ternary alloys, where this anionic competition is absent, the *bowing* character disappears [18].

Conventionally, because of its simplicity, the virtual-crystal approximation (VCA) is preferred for the analysis of chemical disorder in semiconductor alloys. In the VCA, the potential of each atom in the alloy is replaced by a weighted average of the potentials of its components. This method provides a qualitative explanation of most of the features in the bandgap *bowing* of an alloy, however, in systems where large atomic relaxations and reconstructions take place, the VCA vastly underestimates the bowing of the bandgap. In our previous work [17,18,27] the VCA was assumed to be valid, as the lattice-mismatches did not exceed 7%. A more cautious approach is advisable for the GaInN alloys of the present study, as they possess a 10% lattice-mismatch. A critical analysis of the validity and limitations of VCA applied to $Al_xGa_{1-x}As$ alloys was undertaken by Dargam et al. [28] using tight-binding models. These

Table 1
Comparison of the *bowing* parameters in the common-cation compound-semiconductor alloys.

A_xC_1-x alloy	$\Delta a/a_0$	E_g^A (eV)	E_g^C (eV)	B (eV)
$(ZnSe)_x(ZnTe)_{1-x}$[a]	7.3%	2.82	2.39	1.413
$(CdSe)_x(CdTe)_{1-x}$[a]	6.4%	1.71	1.47	0.916
$(GaAs)_x(GaSb)_{1-x}$[b]	7.5%	1.52	0.81	1.294
$(InAs)_x(InSb)_{1-x}$[b]	6.7%	0.42	0.24	0.60

[a] Ref. [17].
[b] Ref. [27].

authors claimed that VCA violation was responsible for the theoretical deviation in predicting the critical aluminum concentration x_c corresponding to the direct-to-indirect bandgap transition.

In situations where the atomic relaxation effects are critically important, the *first principles* methods are ultimately the most reliable in predicting the properties of alloys. For example, *bowing* in the GaInN alloys was studied using *first-principles* pseudo-potential (PP) plane-wave calculations by Ferhat et al. [29,30]. These authors reported that the *bowing* parameter of cubic $Ga_{1-x}In_xN$ alloys is not a constant, rather it depends on the In concentration, i.e., $B = B(x)$. (For instance, $B = 1.61$ eV for $x = 0.25$ and varies to $B = 1.26$ eV for $x = 0.75$.) These latter authors further demonstrated that the *bowing* parameter is controlled by three main parameters: (i) volume deformation (VD), (ii) charge exchange (CE) and (iii) structural relaxation (SR) effects, so that $B = B_{VD} + B_{CE} + B_{SR}$. The VD term represents the relative response of GaN and InN to hydrostatic pressure. The CE term is related to a charge transfer at constant bond length. The SR term describes the change of the bandgap upon passing from the unrelaxed to the relaxed alloy. The strongest contribution to the bandgap *bowing* was found to be the structural effect. Ferhat et al. [29] reported that the Stokes shift between emission and absorption in GaInN alloys is strong, in the order of 200 meV, and is also due to composition fluctuations. It has been confirmed that these latter effects induce the alloy lattice constant to deviate from Vegard's law [30–32]—a clear indication of the VCA violation. In agreement with the above results, Moses and Van de Walle [33] used the state-of-the-art *ab initio* method to show that a composition-independent bowing parameter cannot describe the gap variation in the GaInN alloys. They found a strong bowing for low indium contents, with $B = 2.29$ eV at $x = 0.06$ and $B = 1.79$ eV at $x = 0.125$. They also reported a linear dependence of the valence-band offset (VBO) on the In content. For the average of the top-valence-band states, the VBO was estimated to be about 0.62 eV, which corroborates the experimental one of King et al. [34].

From another perspective, the various sophisticated tight-binding (TB) models have been extensively used to study the electronic and optical properties of disordered systems and alloys [35–40]. In the Slater–Koster scheme [35] the system is described by a Hamiltonian of minimal basis set, and this makes the method capable of dealing with large systems that include thousands of atoms. Since its foundation by Löwdin [36], the development of the TB parametrization has passed through several stages. Vögl et al. [37] added an artificially excited state s^* to the sp^3-basis set of semiconductors to accurately achieve the correct fitting of band dispersions and bandgap energy of the experimental data of pure IV and III–V materials. Prior to this work, Kobayashi et al. [38] used the sp^3s^* models and successfully incorporated the spin–orbit (SO) interaction in their investigation of II–VI materials, such as CdTe and HgTe, for which the SO is of crucial importance. Indeed, such extensions have led to an improvement in the fitting of the valence bands (VBs) and low-energy lying conduction bands (CBs), and also to the inclusion of high-energy lying CBs in the fitting. In case where SO-interactions may be neglected (e.g., silicon), another refinement has been provided by TB models that carry overlap interactions up to the second nearest neighbors [39] and even up to the third nearest neighbors [40]. The main idea is to explore the possible role of other parameters to obtain the best least-square fittings.

In some cases the d-states participate in the bonding and consequently affect the total energy, as in the Ga 3d and In 4d states [41–43]. An extension to accommodate the d-states in the TB-Hamiltonian basis set ($sp^3d^5s^*$) within the framework of nearest-neighbor interaction was first performed by Jancu et al. [43]. Subsequently, the same group extended the scheme to incorporate the SO-interaction in nitride semiconductors (AlN, GaN and InN) for both the cubic zincblende (ZB) and hexagonal wurtzite (WZ) phases [44]. The involvement of the d-states in the bonding is

Table 2
The calculated bandgap energies (E_g), carrier effective masses (m_e and m_h in units of free-electron mass and along the $\langle 1\,0\,0 \rangle$ direction) and spin–orbit coupling energy (Δ_0) are compared to the experimental data of Ref. [2] for zincblende compounds.

Compound	E_g (eV)	m_e	m_h	Δ_0 (eV)	E_g (eV) [a]	m_e [a]	m_h [a]	Δ_0 (eV) [a]
GaN	3.30	0.128	0.220	0.018	3.30	0.15	0.29	0.017
InN	0.72	0.046	0.323	0.010	0.78	0.07	0.30	0.005

[a] Experimental data due to Ref. [2].

Table 3
The sp^3s^* tight-binding parameters, with the inclusion of spin–orbit interaction for both zincblende GaN and InN. These parameters were developed by the authors of Ref. [45].

Compound	E_s^a	E_p^a	E_s^c	E_p^c	E_{s*}^a	E_{s*}^c	λ_a	λ_c
GaN	−12.916	3.270	−1.584	9.130	14.0	14.0	0.003	0.015
InN	−12.861	2.708	−0.399	8.752	15.0	15.0	0.003	0.002

Compound	a_0	$4V_{s,s}$	$4V_{x,x}$	$4V_{x,y}$	$4V_{s,p}^{a,c}$	$4V_{p,s}^{a,c}$	$4V_{s*,p}^{a,c}$	$4V_{p,s*}^{a,c}$
GaN	4.50	−8.900	5.464	8.721	6.715	−7.352	7.844	−2.383
InN	4.98	−4.229	4.868	6.750	3.323	−5.609	8.976	−3.051

essential, especially if hydrostatic pressure is applied. However, in optimizing the basis set, many other TB-models have excluded the d-states in the analysis of freely strained nitride alloys. This latter scheme, with the inclusion of SO-interactions, nevertheless yields estimates of band dispersions and bandgap energy in favorable agreement with the experimental data [45] (see Table 2).

In the present contribution two unusual features of cubic $Ga_{1-x}In_xN$ ternary alloys are investigated. The first is that these common-anion ternary alloys are expected to lack or to have a very weak *bowing* character. Surprisingly, the alloys were found to possess strong *bowing* character. The origins of the unexpected *bowing* characteristics are part of this study. The second is that the *bowing* parameter shows composition-dependence deserving further inspection. The present work employs the sp^3s^* TB method, which includes the SO coupling within the VCA framework to calculate the band structures, PDOS, TDOS, charge ionicities versus both composition and VBO. The results will be compared to some recently available experimental optical absorption (Abs) and photoluminescence (PL) data.

This paper is organized as follows. An overview of the TB method is given in Section 2. In Section 3 the results are discussed and their uses in modeling the PL and Abs data are demonstrated. Finally, in Section 4 the main findings and conclusions are summarized.

2. Computational method

The present work utilizes the sp^3s^*-TB-models with the inclusion of the spin–orbit coupling, developed by Hernandez-Cocoletzi et al. [45]. Great efforts by these latter authors were focused on the fitting of the valence-bands (VBs) and low-energy-lying conduction bands (CBs) [45], while the bandgap energy and carrier effective masses were fit to the experimental data. For completeness, the TB parameters are shown in Table 3. Moreover, in the supercell calculations, dealing with alloy structures, the validity of two main points is assumed: (i) the VCA in evaluating the supercell atomic structure. The energy error-bar in such calculations due to the neglect of atomic relaxations will be estimated; and (ii) the problem of energy reference between the alloy constituents is sorted out by taking the VBO between various materials into account [17]. For instance, in the present case, the valence band edge of InN stands higher in energy than that of GaN when an interface is formed between these two materials [46]. Namely, in the case of a free-standing heterostructure, the $\text{VBO} = E_v(\text{InN}) - E_v(\text{GaN}) \geq 0$. Consistent with this point as well as with the VCA principle, is the case of $Ga_{1-x}In_xN$ alloy, as each In-atom is bonded to four N-atoms, all the In on-site energies are shifted by VBO value. However, each N-atom is fourfold coordinated with x fraction to be In and $(1 - x)$ fraction to be Ga. Hence, the N on-site energies are shifted by $(x \times \text{VBO})$ with respect to the bulk values. According to the *first-principles* all-electron band-structure calculations, the VBO values were reported by Wei and Zunger [46] to be about 0.26 eV, and recently by Li et al. [47] to be 1.11 eV. This latter value represents the highest value, that can be found in literature, and should be considered as an upper estimate.

Within the linear-combination of atomic orbitals (LCAO) basis set representation, the TB Hamiltonian is diagonalized. The obtained eigen-energies $E_{n\mathbf{k}}$ and the corresponding eigen-functions $|n, \mathbf{k}\rangle$ (Bloch functions) are used to calculate the following quantities:

(i) the total density of states (TDOSs) is given by:

$$N(E) = \frac{1}{N_W} \sum_{n,\mathbf{k}}^{N_W} \delta(E - E_{n\mathbf{k}}) \quad (1)$$

where N_W is the number of $\mathbf{k}$-vectors taken from within the irreducible wedge (IW) of the Brillouin zone (BZ); n is a band index; $\mathbf{k}$ is a wave-vector taken from within the IW. We quote that $N_W = 200$ is found to be sufficient to secure the convergence of DOS and charge calculations in the case of a supercell of one-unit-cell size (i.e., containing 8 atoms);

(ii) the local density of states (LDOS), due to the orbital μ on the atom b, is given by:

$$N_{b,\mu}(E) = \frac{1}{N_W} \sum_{n,\mathbf{k}}^{N_W} |\langle b, \mu, \mathbf{R_i} | n, \mathbf{k} \rangle|^2 \delta(E - E_{n\mathbf{k}}) \quad (2)$$

where $\mathbf{R_i}$ is the position vector of atom b;

(iii) the partial density of states (PDOSs), due to the atomic species of type α (such as Ga, In or N atoms), is given by:

$$N_\alpha(E) = \sum_{b,\mu} N_{b,\mu}(E) \quad (3)$$

where the sum of b runs over all sites of type α.

We emphasize that the $\mathbf{k}$-space integration, carried out in evaluating Eqs. (1) and (2), is performed using the Monkhorst–Pack technique [48], and the δ-function is numerically approximated by a Gaussian:

$$\delta(x) = \frac{1}{\sigma\sqrt{2\pi}} \exp\left[-\frac{x^2}{2\sigma^2}\right] \quad (4)$$

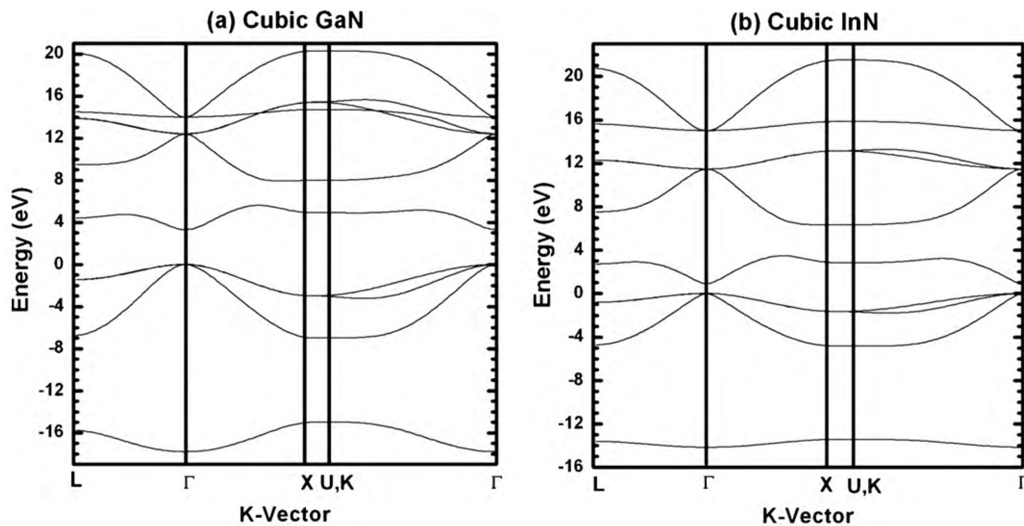

Fig. 2. Band structures of zincblende phases of: (a) GaN and (b) InN.

of width $\sigma = 0.10$ eV to smear out the effects of discreteness of the BZ sampling and experimentally to take account of the thermal broadening. All the calculated TDOSs are normalized to 10 electrons (i.e., electronic content of one atom);

(iv) the electric charge of the upper shell of an individual atom using its PDOS is given by:

$$q_\alpha = \frac{4e}{\rho} \int_{E_{min}}^{E_F} N_\alpha(E)dE \quad (5)$$

where e is the electron charge; q_α is expressed in absolute e-units; the number 4 in the equation arises from spin degeneracy and renormalization of the density over one molecule; ρ is the atomic mole fraction (for instance in the case of $Ga_{1-x}In_xN$ alloy, $\rho = 1 - x, x$, or 1 corresponding to Ga, In or N, respectively); E_{min} is any energy value below all state levels forming the TDOS; and E_F is the Fermi energy which is taken to be equal to $E_g/2$, which is assumed in the case of frozen-lattice state ($T = 0$ K);

(v) the ionization of each constituent atom. For instance, if we consider AB as a III–V semiconductor compound, then the ionizations of A (3-valency atom) and B (5-valency atom) are defined as: $I_A = 3 - q_A$ and $I_B = 5 - q_B$ are expressed in absolute-electron charge $|e|$ units.

3. Results and discussion

3.1. Binary-compound electronic structure

Fig. 2 shows the respective band structures of the cubic phases of (a) GaN and (b) InN. Each panel shows ten spin-degenerate bands among which four consist the VBs and the remaining six form the CBs. The VB-edge is taken as an energy reference. It is clear that the SO-interaction is negligible in both GaN and InN, as the triplet state at the top of VB at the Γ-point is not split. This triplet is composed by light-hole (LH), heavy-hole (HH) and spin-off states. The energy gaps for GaN and InN are direct (at Γ-point) and their respective values are: $E_g = 3.30$ eV and 0.72 eV, which completely agree with the experimental data (see Table 2). In either panel 2a or b, the lowest group is dominated by the contribution from the s-orbitals of anions (nitrogen atoms). The second group, which forms the VB, consists of the cationic s states and all the p states. The third group of bands, which form the CB, are mainly due to contributions from the p and cationic s states as anti-bonding states to the VB. The highest-energy CBs are dominated by the s* states. One may notice the splitting of CB into two groups for GaN and even three groups for InN while the attention was fully focused, in Ref. [45], on producing the best VBs and the best low-energy-lying CBs as fitted to experimental data.

Fig. 3 illustrates the TB-results of density of electronic states for both (a) GaN and (b) InN in their zincblende crystal structures. Each panel shows the TDOS and its components made of the PDOSs due to the constituent atoms. The VB-edge is taken as an energy reference and the TDOS is normalized to 10 electrons (per atom). In Fig. 3a, by comparing the PDOS contributions of Ga and N-atoms, one can clearly notice that the overall magnitude of VB of Ga-atoms is smaller than that of N-atoms; and conversely, the overall magnitude of CB of Ga-atoms is larger than that of N-atoms. This fact reveals that the GaN is a polar material as the charge of the chemical bond has the tendency to accumulate near N atom more than the Ga-atom. As a matter of fact, the charges of Ga and N are found to be $q_{Ga} = 2.71e$ and $q_N = 5.29e$. Consequently the respective charge ionicities of these latter atoms would be $I_{Ga} = +0.29e$ and $I_N = -0.29e$, which indeed indicate that N is electronegative and Ga is electropositive. Fig. 3b shows similar trends for InN as those previously discussed for GaN. The overall magnitude of VB of N-atoms looks much larger than that of In-atoms. The respective charge ionicities are $I_{In} = +0.624e$ and $I_N = -0.624e$. Here, one can clearly notice that the ionicity of N-atom in InN is larger than the one of N-atom in GaN. This reveals that the InN is more polar than GaN, as the In-atom being more electropositive than the Ga-atom. It is expected that the competition between these charge polarities will play a major role in producing the "*bowing*" character in the $Ga_{1-x}In_xN$ alloys.

3.2. Ternary-alloy DOS

Fig. 4 displays the calculated TDOSs and PDOSs for the ternary $Ga_{1-x}In_xN$ alloys with increasing indium content: (a) $x = 0.25$, (b) $x = 0.50$, and (c) $x = 0.75$. In each case, the VB-edge is taken as an energy reference and both the VB-edge and the CB-edge are indicated by the shown-vertical dotted lines. As mentioned in the previous section, TDOS is normalized to 10 electrons (which is the total number of input basis-set states per atom in the Hamiltonian). Fig. 4 used VBO = 0.26 eV, which was obtained by Wei and Zunger [46]. Furthermore, Fig. 4 focuses on the near-gap energy region within 6.0 eV around the VB-edge as to study the variation of valency states versus indium content. We start by looking at the TDOS variation versus indium content x. The increase of the CB with increasing x reveals that the In-atoms are more electropositive than

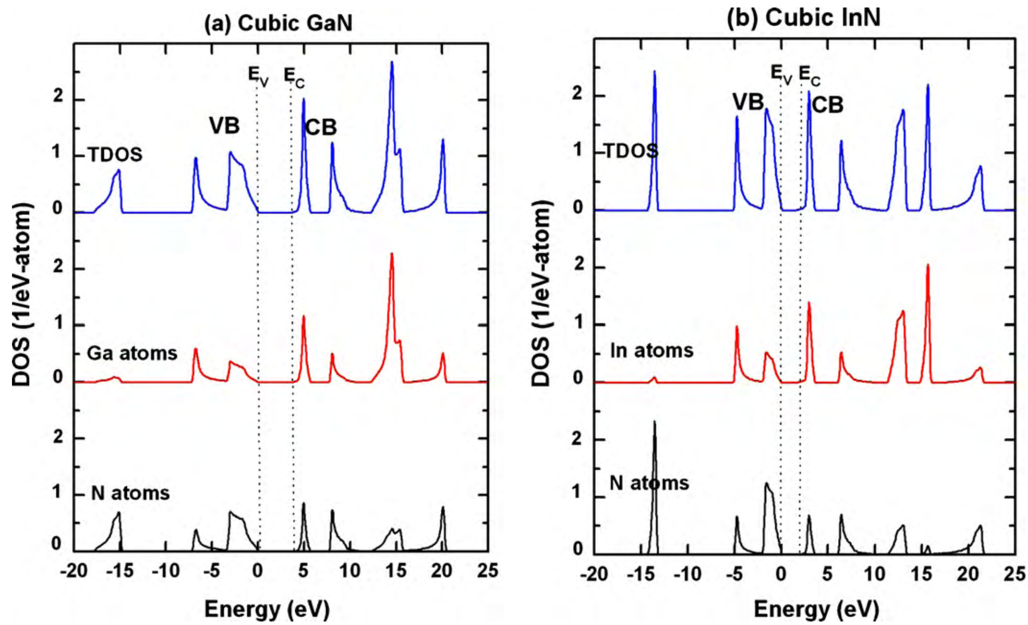

Fig. 3. TDOS and its PDOS components for zincblende bulk structures: (a) GaN and (b) InN. The VB-edge is taken as an energy reference.

the Ga-atoms and, thus, more ionization of nitrogen atoms should be expected. By comparing the PDOSs of Ga-atoms and In-atoms within VBs ($E \leq 0$ eV), especially at a concentration of $x = 0.50$, one can clearly notice the arrangement taking place between the two cations in filling the VB-states and, consequently, in the compromise in losing their charges. Lastly, in the PDOS of N-atoms, one may notice the growth of the overall magnitude of VB with the increasing indium content. This reveals that N-atoms are getting more negatively ionized with the increasing In content. Therefore, it is interesting to analyze the variation of ionicity of each atomic species in the alloy versus In content.

3.3. Ternary-alloy charge ionicity

The total charge on the upper shell of each constituent atom in the alloy is calculated by integrating its corresponding PDOS up to the Fermi level, as it has been described in the previous section. From the calculated charge, the ionicity of each atom is calculated and presented in Fig. 5. Three different VBO values are considered and presented in different panels: (a) VBO = 0 eV, which is usually predicted by the well-known common-anion rule of heterostructures; (b) VBO = 0.26 eV, which was obtained by Wei and Zunger [46] using the first-principles all-electron band-structure method; and (c) VBO = 1.11 eV, which was recently obtained by Li et al. [47] using the same preceding method but by taking into account the deformation potential of core states. The charge ionicities of atomic species in the $Ga_{1-x}In_xN$ alloy are indicated by the following symbols: open circles for N-atom; full triangles for Ga-atom; and full squares for In-atom. The charge neutrality is well fulfilled in every case, namely, as:

$$I_N + (1 - x)I_{Ga} + xI_{In} = 0 \quad (6)$$

where I_N, I_{Ga} and I_{In} are the atomic-charge ionicities of N-, Ga- and In-atoms, respectively.

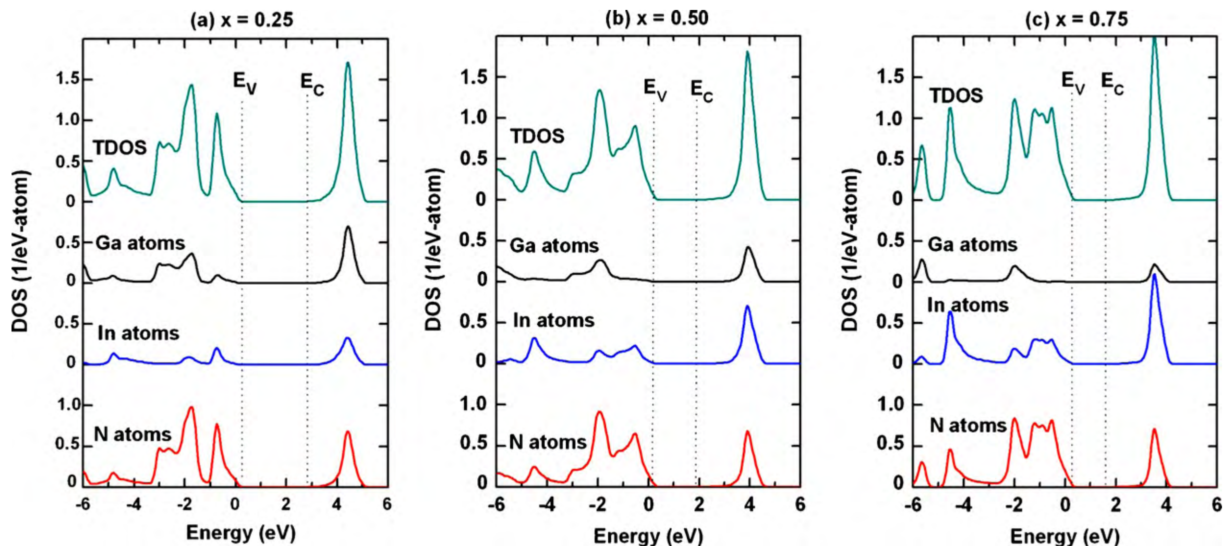

Fig. 4. TDOS and its PDOS components calculated for $Ga_{1-x}In_xN$ alloys with: (a) $x = 0.25$; (b) $x = 0.50$ and (c) $x = 0.75$. The VB- and CB-edges (E_v and E_c) are shown by the dotted vertical lines and the VB-edge is taken as an energy reference ($E_v = 0$).

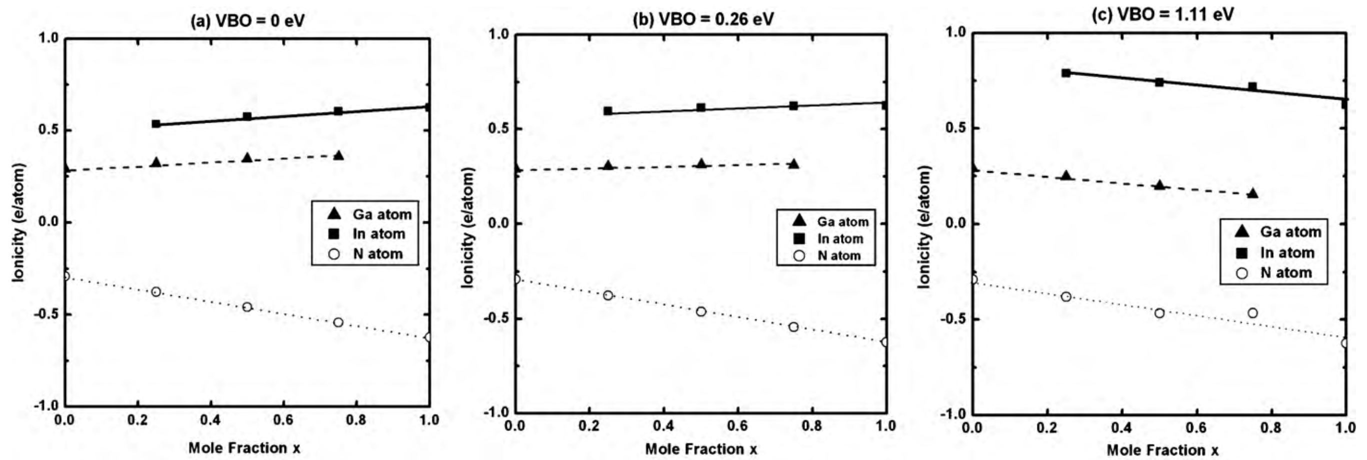

Fig. 5. The variation of charge ionization with mole fraction x for the constituent atoms of the $Ga_{1-x}In_xN$. Different values of VBO are considered: (a) VBO = 0 eV, (b) VBO = 0.26 eV, and (c) VBO = 1.11 eV.

Furthermore, in all three panels, the charge variation of nitrogen atom in the $Ga_{1-x}In_xN$ alloy seems to be linear and independent of VBO. In contrast, the ionicities of cation atoms (Ga and In) are found to be sensitive to VBO. Meanwhile, there exists a critical value of VBO (hereafter denoted by V_c) at which the slopes of ionicities of the latter two atoms change from being positive (Fig. 5a) to negative (Fig. 5c). It is noticeable that the ionicities of Ga and In follow the same variation as their corresponding curves are parallel (i.e., having the same slope). The rule of variation of the charge ionicities may be written as:

$$I_N = -0.29(1-x) - 0.624x \tag{7}$$

$$I_{Ga} = sx + 0.29 \tag{8}$$

$$I_{In} = s(1-x) + 0.624 \tag{9}$$

where s is the slope: $s = 0.313(V_c - \text{VBO})$, with $V_c = 0.384$ eV. At this latter critical VBO value (i.e., VBO $= V_c$), the ionicities of Ga and In-atoms in the alloy are supposed to remain constant as in their corresponding bulk structures. This latter is not really a favorable case as the Ga and In-atoms possess different electronegativity characters and should rather couple to N in different ways. A competition in losing their charges especially in the presence of very strong electronegative anion atoms, such as N-atoms, is very much expected. So, the slope "s" should be either positive or negative. For VBO $> V_c$ (as in Fig. 5c), to expect the In-atom to loose charge more than its state in the bulk InN, while the Ga-atom to loose less charge than its state in the bulk GaN, is not really a probable case. On the other hand, for VBO $< V_c$ (as in Fig. 5a and b), a compromise between the cation atoms (Ga and In) in losing their charges to the nitrogen atoms would be more physically favorable. So, our TB-calculation indicates VBO will be small in the present case of $Ga_{1-x}In_xN$ alloys (i.e., VBO < 0.38 eV). This is not only based upon the present discussion of the charge ionicity variation but also upon the modeling of the experimental data, which will be shown in next sub-section. Besides the fact that small or vanishing VBO values are consistent with the predictions of the common-anion rule.

3.4. Modeling of experimental data

Using molecular-beam epitaxy (MBE), high-quality In-rich $Ga_{1-x}In_xN$ films ($0.5 \le x \le 1.0$) were grown on sapphire substrates [10], employing either an GaN or InN buffer layer and producing WZ alloys. The optical properties of the produced samples were characterized by optical absorption and photoluminescence spectroscopy at about 80 K. Based on the Abs data, with the exclusion of their proper PL data, besides using some experimental data of Ga-rich alloys (namely, due to the bandgap energy measurements by photo-modulated transmission [49] and optical absorption [50]), a *bowing* parameter $B = 1.43$ eV was reported). However, one should emphasize here that if the PL data of Wu et al. [10] corresponding to the In-rich alloys were also included in the fitting, the *bowing* parameter would have been much greater than the preceding reported value. The entire data produced in Ref. [10] are displayed in Fig. 6 by open triangles.

More recently, Franssen et al. [11] reported their experimental results of pressure-dependence of PL of $Ga_{1-x}In_xN$ films in the full composition range $0 \le x \le 1$ at 80 K. Their PL data are shown in Fig. 6 in open circles. They confirmed the clear deviation from the linear to the *bowing* behaviors with a parameter B even larger than the one reported by Wu et al. [10]. In Fig. 6a, we assumed a single *bowing* parameter to fit each theoretical or experimental data. For the displayed experimental data, we have performed a non-linear fitting using the functional form:

$$E_g = xE_g^{InN} + (1-x)E_g^{GaN} - Bx(1-x) \tag{10}$$

where we took $E_g^{GaN} = 3.30$ eV and $E_g^{InN} = 0.72$ eV. In Fig. 6a, the result of the fitting of the optical absorption data, shown in dotted line, yields a bowing parameter $B = 1.703$ eV. Whereas the fitting of the PL data [11], shown in small-dashed curve, yields $B = 2.297$. On the other hand, our TB-theoretical calculations were carried out using VBO = 0.26 eV, after a bit acting on one TB (E_p^a) to yield the preceding experimental bulk bandgap energies for GaN and InN. The TB-results are shown in Fig. 6a by crosses. Using the above functional form, the best fit to our TB-results is shown in solid line and yielding $B = 1.644$ eV, in excellent agreement with the Abs data. The PL data seem to predict an even higher *bowing* parameter and smaller VBO than 0.26 eV (see below). Consequently, the data shown in Fig. 6a provide experimental evidence for the clear deviation from linearity to clear *bowing* character. Meanwhile, one may notice that TB result (cross) at $x = 0.25$ lies below the solid line of TB fitting; whereas the cross at $x = 0.75$ lies above the same solid line. This may reveal that the TB-results corroborate the idea of *bowing* enhancement in the region of low In content. As a matter of fact the PL data, in the region of low In content, lie much below all fitting curves and reveal high *bowing* parameter. Here, it is worth trying to apply a composition-dependent *bowing* parameter, which decreases with the increasing In content.

It is worth noting the clear discrepancy between the PL and Abs experimental data. This discrepancy is known by the Stokes shift

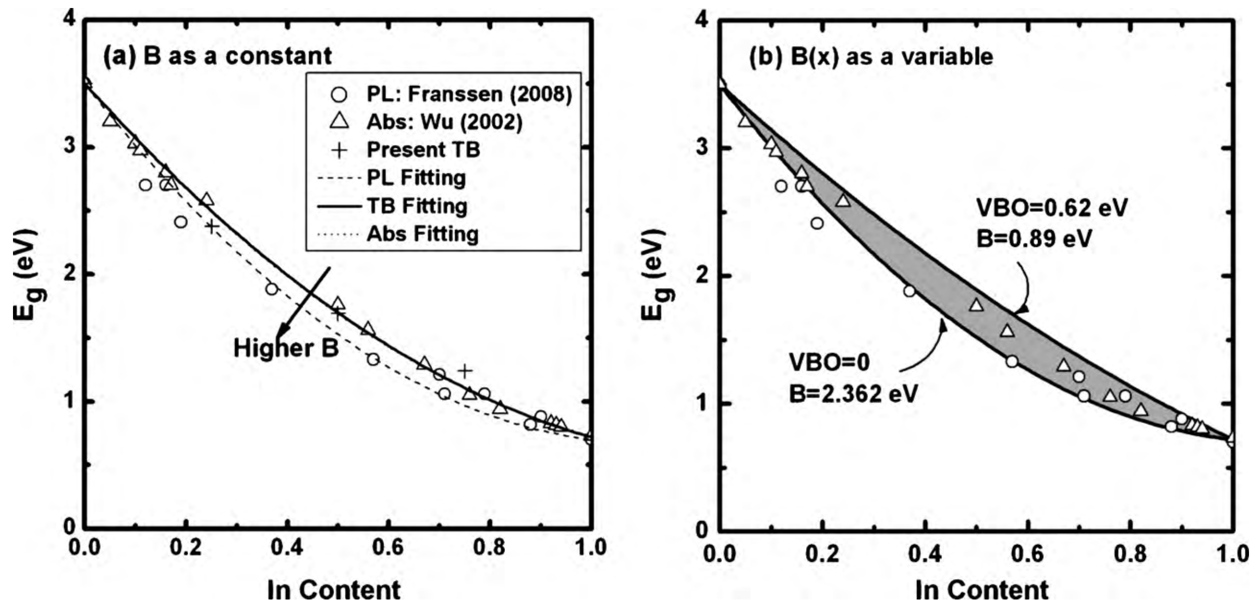

Fig. 6. Comparison of the present TB-results, of $E_g(x)$ in the $Ga_{1-x}In_xN$ alloys, to the experimental optical absorption and PL data. (a) B is constant and (b) $B = B(x)$ is as a variable.

between absorption and emission spectra. Stokes shift might be a negative indicator of the quality of grown samples. From a theoretical point of view, it is not completely clear the origin of the Stokes shift, even if many models have been proposed [29,51,52]. It is generally observed with stronger effect for smaller nanocrystals or quantum dots [53]. In the experimental data shown in Fig. 6, the Stokes shift can reach 200 meV in consistency with the *ab initio* calculations of Ferhat et al. [29]. The formation of InN clusters (dot-like) should enhance the formation and recombination of the electron–hole pairs and the Stokes shift might be an indicator to that structural heterogeneity.

In our modeling, to assess the relaxation effects, we present in Fig. 6b two extremum cases of VBO. The smallest value VBO = 0, which is predicted by the common-anion rule. From there, we maximize the value of the *bowing* parameter by taking the one corresponding to lower In concentration ($x = 0.25$). On the other hand, the largest value VBO = 0.62 eV, which was recently reported by Moses and Van de Walle [33]. From which we minimize the value of the *bowing* parameter by taking the one corresponding to the high In concentration ($x = 0.75$). The curves corresponding to these latter two *bowing* parameters are shown in Fig. 6b with a shaded area in between them. It is clear that the *bowing* parameter cannot be less than about 1.0 eV. However it should even exceed 2.362 eV particularly for low In content. The shaded area might represent the TB-theoretical error-bar accounting for the lattice relaxation and the deviation from the VCA validity.

Fig. 7a shows the TB-results of *bowing* parameter versus VBO for different In contents: $x = 0.25$, 0.50 and 0.75. It shows that B decreases linearly with VBO (i.e., $B = aV + b$, where V is the VBO, a and b are constants with a being the negative slope). More importantly, Fig. 7a shows the lines to be parallel and almost equidistant, revealing a linear decrease of B versus the In content (x). In fact, Fig. 7b displays the variation of *b* owing parameter B versus the In content (x) for various VBO values. It confirms the linear decrease of B versus In content (i.e., $B = cx + d$, where c and d are constants with c being the negative slope). Thus, one can deduce a linear increase of

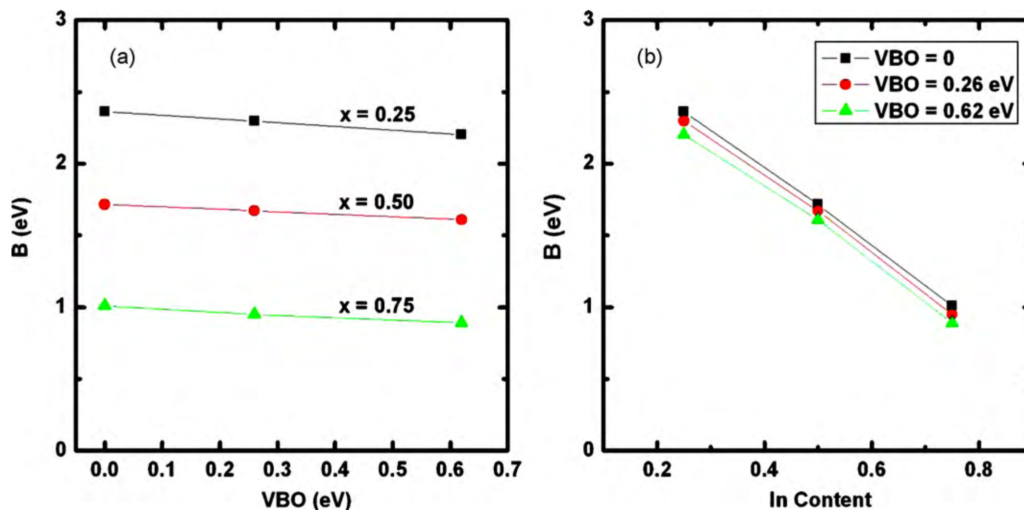

Fig. 7. (a) The TB-calculated *bowing* parameter "B" of $Ga_{1-x}In_xN$ alloys versus VBO for various In contents and (b) B versus In content for various VBO values.

Table 4
Bowing parameter (B) versus element electronegativity (χ)in the common-anion alloys. The unit of χ is taken to be "Pauling".

Group	Alloy	$\Delta a/a_0$	B (eV)	χ_{ave}^{cation} (Pauling) [f]	χ^{anion} (Pauling) [f]
II–VI	CdZnSe	7.0%	$\ll$0.3 [a]	1.67	2.55
	CdZnTe	6.5%	$\ll$0.3 [a]	1.67	2.10
III–V	GaInAs	6.8%	0 [b]	1.79	2.18
	GaInSb	6.0%	0 [b]	1.79	2.05
	GaInN	10%	1.43 [c], 1.64 [d], 1.70 [e]	1.79	3.04

[a] Ref. [18].
[b] Ref. [54].
[c] Ref. [10].
[d] Present work.
[d] Ref. [11].
[f] Ref. [55].

VBO versus In content (i.e., $B = aV + b = cx + d$, which implies that V ($\equiv$VBO) increases linearly with x as long as a and c are both negative constants). This latter variation is consistent with the recent *ab initio* results of Moses and Van de Walle [33].

Lastly, Table 4 summarizes the electronegativity of the anions in some common-anion alloys. It is clear that nitrogen possesses much higher electronegativity and should be the driving force enhancing somewhat like a compromise between cations in losing their charges with the increasing In content in the $Ga_{1-x}In_xN$ alloys.

4. Conclusions

The origins of the existence of the *bowing* character in $Ga_{1-x}In_xN$ were investigated using the sp^3s^* tight-binding method, with the inclusion of spin–orbit coupling affects and within the VCA framework. The theoretical TB modeling of the experimental optical absorption [10] and the recent photoluminescence [11] data confirmed that these alloys possess a clear *bowing* character. Two unusual characteristics were analyzed:

(i) while the common-anion "direct-bandgap-based" ternary alloys lack or have a very weak *bowing* character, the GaInN alloys are found to possess an obvious "*bowing*". The present study shows that this behavior is mainly a result of the pronounced electronegativity of the nitrogen atoms. This feature can induce a competition between the cation (Ga and In) atoms to establish a compromise ionization with the increasing indium content;

(ii) a single composition-independent value for the *bowing* parameter cannot describe the bandgap behavior. The decrease in the *bowing* parameter with increasing In content is probably caused by composition fluctuation due to considerable lattice relaxation in the alloy that correlates with their degree of lattice mismatch. B is found to decrease linearly with the In content and to also linearly decrease with VBO. The best fit of the experimental data requires higher B (smaller VBO) in the Ga-rich region and smaller B (larger VBO) in the In-rich region. One can easily deduce that VBO increases linearly with the In content (x), which is in excellent agreement with the recent *ab initio* results of Ref. [33].

The modeling also suggests that the VBO is small between the two alloy constituents (i.e., VBO < 0.38 eV), which is consistent with the prediction of the common-anion rule and the findings of the state-of-the-art *ab initio* calculations [46].

Acknowledgments

The author is indebted to Stacey Lee Patton and Drs. John Graham, Jeams Tomas Fowler and El-Hadi Sadqi for their critical readings of the manuscript. This work is partially supported by the Research Affairs of the UAE University, under grant number 08-02-2-11/09.

References

[1] S. Adachi, in: P. Capper, S. Kasap, A. Wiloughby (Eds.), Properties of Semiconductor Alloys: Group-IV, III–V and II–VI Semiconductors, John Wiley, Wilshire, UK, 2009.
[2] I. Vurgaftman, J.R. Meyer, J. Appl. Phys. 94 (2003) 3675.
[3] M.C. Amann, F. Capasso, A. Larsson, M. Pessa, New J. Phys. 11 (2009) 125012.
[4] L.D. Yao, et al., J. Alloys Compd. 490 (2009) 798.
[5] V.R. D'Costa, et al., Phys. Rev. B 73 (2006) 125207.
[6] C. Persson, O. Nur, M. Willander, E.A. de Andrada e Silva, A.F. da Silva, Brazil. J. Phys. 36 (2006) 447.
[7] P. Moontragoon, et al., Semicond. Sci. Technol. 22 (2007) 742.
[8] W. Lu, et al., Semicond. Sci. Technol. 24 (2009) 105016.
[9] S.R. Bank, H.B. Yuen, H. Bae, M.A. Wistey, J.S. Harris, Appl. Phys. Lett. 88 (2006) 221115.
[10] J. Wu, W. Walukiewicz, K.M. Yu, J.W. Ager, E.E. Haller, H. Lu, W.J. Schaff III, Appl. Phys. Lett. 80 (2002) 4741.
[11] F. Franssen, et al., J. Appl. Phys. 103 (2008) 033514.
[12] M. Zhu, et al., Phys. Rev. B 81 (2010) 125325.
[13] D.A. Contreras-Solorio, J. Madrigal-Melchor, S.J. Vlaev, A. Enciso, H. Hernandez-Cocoletzi, Microelectron. J. 39 (2008) 435.
[14] A. Yoshikawa, S. Che, Y. Ishitani, X. Wang, J. Cryst. Growth 311 (2009) 2073.
[15] S. Che, A. Yuki, H. Watanabe, Y. Ishitani, A. Yoshikawa, Appl. Phys. Express 2 (2009) 021001.
[16] S. Schulz, et al., Phys. Status Solidi C 3 (2006) 3827.
[17] N. Tit, I.M. Obaidat, H. Alawadhi, J. Phys.: Condens. Matter 21 (2009) 075802.
[18] N. Tit, I.M. Obaidat, H. Alawadhi, J. Alloys Compd. 481 (2009) 340.
[19] A. Rogalski, J. Antoszewski, L. Faraone, J. Appl. Phys. 105 (2009) 091101.
[20] A. Lindsay, E.P. O'Reilly, Phys. Status Solidi C 5 (2008) 454.
[21] I. Vurgaftman, J.R. Meyer, J. Appl. Phys. 94 (2003) 3675.
[22] N. Tit, M.W.C. Dharma-wardana, Appl. Phys. Lett. 76 (2000) 3576.
[23] N. Tit, J. Phys. D: Appl. Phys. 39 (2006) 2514.
[24] K. Kim, L.W. Hart Gus, A. Zunger, Appl. Phys. Lett. 80 (2002) 3105.
[25] S.H. Wei, A. Zunger, Phys. Rev. B 39 (1989) 6279.
[26] S.H. Wei, A. Zunger, Phys. Rev. B 55 (1997) 13605.
[27] N. Tit, N. Amrane, A.H. Reshak, J. Electron. Mater. 39 (2010) 178.
[28] T.G. Dargam, R.B. Capaz, B. Koiller, Braz. J. Phys. 27A (1997) 299.
[29] M. Ferhat, J. Furthmüller, F. Bechstedt, Appl. Phys. Lett. 80 (2002) 1394.
[30] M. Ferhat, F. Bechstedt, Phys. Rev. B 65 (2002), 075213–1/7.
[31] Y.K. Kuo, B.T. Liou, S.H. Yen, H.Y. Chu, Opt. Commun. 237 (2004) 363.
[32] S. Saib, N. Bouarissa, P. Rodriguez-Hernandez, A. Munoz, J. Phys.: Condens. Matter 19 (2007) 486209.
[33] P.G. Moses, C.G. Van de Walle, Appl. Phys. Lett. 96 (2010) 021908.
[34] P.D.C. King, et al., Phys. Rev. B 78 (2008) 033308.
[35] J.C. Slater, G.F. Koster, Phys. Rev. 94 (1954) 1498.
[36] P.O. Löwdin, J. Chem. Phys. 18 (1950) 365.
[37] P. Vögl, H.P. Hjalmarson, J.D. Dow, J. Phys. Chem. Solids 44 (1983) 365.
[38] A. Kobayashi, O.F. Sankey, J.D. Dow, Phys. Rev. B 25 (1982) 6367.
[39] G. Grosso, C. Piermarochhi, Phys. Rev. B 51 (1995) 16772.
[40] Y.M. Niquet, C. Delerue, G. Allan, M. Lannoo, Phys. Rev. B 62 (2000) 5109.
[41] W.R.L. Lambrecht, B. Segall, S. Strite, G. Martin, A. Agarwal, H. Markoc, A. Rockett, Phys. Rev. B 50 (1994) 14155.
[42] A. Qteish, A.I. Al-Sharif, M. Fuchs, M. Scheffler, S. Boeck, J. Neugebauer, Comp. Phys. Commun. 169 (2005) 28.
[43] J.-M. Jancu, R. Scholz, F. Beltram, F. Bassani, Phys. Rev. B 57 (1998) 6493.
[44] J.-M. Jancu, F. Bassani, F. Della Sala, R. Scholz, Appl. Phys. Lett. 81 (2002) 4838.
[45] H. Hernandez-Cocoletzi, D.A. Contreras-Solorio, S.J. Vlaev, A. Enciso, I. Rodriguez-Vargas, Physica E 41 (2009) 1466.
[46] S.-H. Wei, A. Zunger, Appl. Phys. Lett. 72 (1998) 2011.
[47] Y.-H. Li, et al., Appl. Phys. Lett. 94 (2009) 212109.
[48] H.J. Monkhorst, J.P. Pack, Phys. Rev. B 13 (1976) 5188.
[49] W. Shan, et al., J. Appl. Phys. 84 (1998) 4452.

[50] S. Pereira, M.R. Correia, T. Monteiro, E. Pereira, E. Alves, A.D. Sequeira, N. Franco, Appl. Phys. Lett. 78 (2001) 2137.
[51] F. Yang, M. Wilkinson, E.J. Austin, K.P. O'Donnell, Phys. Rev. Lett. 70 (1993) 323.
[52] K.P. O'Donnell, R.W. Martin, P.G. Middleton, Phys. Rev. Lett. 82 (1999) 237.
[53] E. Degoli, et al., Phys. Rev. B 69 (2004) 155411.
[54] R. Roucka, J. Tolle, B. Forrest, J. Kouvetakis, V. D'Costa, J. Menendez, J. Appl. Phys. 101 (2007) 013518.
[55] M.V. Putz, Absolute and Chemical Electronegativity and Hardness, Nova Science, New York, 2009.